

Simulation of Ultra-Intense Laser Irradiation Induced High Electronic Excitation of Bandgap Materials

**T. Apostolova¹, P. Detistov¹, M.V. Ivanov¹, Y. Oriault²,
J.M. Perlado², A. Rivera²**

¹Institute for Nuclear Research and Nuclear Energy, Bulgarian Academy of Sciences, Sofia 1784, Bulgaria

²Instituto de Fusión Nuclear, Universidad Politécnica de Madrid, Spain

Abstract. Using a quantum kinetic approach we describe high electronic excitation of fused silica induced by short pulse, intense laser irradiation. We concentrate on the effect of the impact ionization process on the electron density and average kinetic energy of the electron system. In addition the effect of electron-phonon coupling in the material and the subsequent change in lattice temperature are described. It is evident that even at short pulse duration the role of these processes is significant.

1 Introduction

With the advent of affordable Ti: sapphire lasers, several disciplines have benefited to such an extent that many include now the prefix *femto*, *e.g.*, femtochemistry, femtotechnology, femtophotography, femtooptics. In fact, fs-lasers constitute a unique tool to carry out research at the electronic scale because many characteristic lifetimes match typical pulse durations. These short pulses open new possibilities to study phenomena related to high electronic excitation in matter because high intensities are delivered onto easily reachable tiny spots. A myriad of processes occur depending on experimental conditions and irradiated material, *e.g.*, non-linear optical absorption, secondary carrier ionization, non-equilibrium scattering, carrier thermalization and recombination. The results of the different concomitant processes are not at all easy to predict. In some cases, non-permanent effects occur, just transient effects, which significantly affect the optical properties of the irradiated spot. These effects constitute the basis of some applications in the ultra-fast optics field. In some other cases, permanent modifications of the irradiated material take place through plume formation, surface ablation or modification of physicochemical properties. The pulsed nature of fs-laser irradiation makes possible to study the resulting non-equilibrium high electronic density as a function of time with matured pump-probe techniques, which provide very relevant information on the electronic evolution of the sys-

tem. On the other hand, practical codes to model the experiments are still under development due to their complexity.

In this paper we describe a number of relevant microscopic processes in bandgap materials (insulators and semiconductors) with a model based on a quantum formalism described in a previously published work [1]. We focus on the role of impact ionization mechanisms as an additional way to enhance the non-equilibrium electron distribution in the conduction band. In addition, we also show the effect of electron-phonon coupling on energy transfer from the conduction band to the lattice, resulting in an increase of the lattice temperature. The chosen model case to describe the role of these processes is fused silica irradiated with 100 fs laser pulse with different photon energies (laser wavelengths). The relative importance of impact ionization and electron-phonon coupling for different photon energies is demonstrated.

2 Processes during and after a Laser Pulse

In this work, we consider the effects induced by fs-laser pulses on fused silica. Photon energies are chosen significantly smaller than the silica band gap (9 eV). Therefore, photon absorption only takes place through multi-photon ionization (PI) when the laser intensity is sufficiently high. When this is the case, the conduction band gets swiftly populated by quasi-free electrons that in turn can absorb additional photons through the so-called free carrier absorption (FCA) process. This mechanism makes possible that a small but relevant tail of high-energy electrons appear in the non-equilibrium electron distribution. Since electrons in the tail gain kinetic energy in excess of the bandgap they can further ionize the material by impact ionization (II) processes. Typically, with characteristic times longer than the pulse duration, scattering processes, electron-electron (EE) and electron-phonon (EP) tend to relax the electron system. The latter, constitutes an important channel of energy transfer to the lattice and it is in many cases the main channel for lattice heating.

3 Boltzmann Scattering Equation Method

In the field of kinetic models, one starts from Boltzmann-like kinetic (BE) equation and develops complex, yet tractable numerical schemes. Kinetic models like the Master and Boltzmann's equations can be formally derived from the theory of non-equilibrium Green's functions, within the framework of the so-called quasi-particle approximation. These, however, are limited to the semi-classical regime, *i.e.* when the electron-hole plasma dynamics is controlled by collisions (Markovian) rather than by coherent quantum effects. This condition is satisfied in the sub-picosecond regime, with the mean time-independent collision rates calculated via Fermi's golden rule, which implies strict energy conservation. Instead of tracing the motion of the individual particles, one follows the time evolution of the particle distribution function in phase space, starting from the

Liouville equation. Simplifications of the latter lead to Boltzmann-type kinetic equation used in this work to calculate the temporal evolution of the electron distribution corresponding to an energy in excess with respect to the bottom of the conduction band and in order to account for the features of sub-picosecond electronic and structural events described in the previous section.

For the purposes described above the BE for electron distribution function used previously [2] is modified to include terms of time-dependent optical generation rate given in its semi-classical form as, *e.g.*, in reference [3]. In the case of wide band gap dielectrics we include PI directly into the BE [4–6], [1] as well as II and AR. The connection between the electron occupation number, n_k^e , and the electron energy distribution function, f_k^e , is given in reference [7], $f_k^e = \rho_k n_k^e$, where $\rho_k^e = C_0 \sqrt{E_k}$ is the reciprocal density of states with $C_0 = (2m_e^*)^{3/2} (2\pi^2 \hbar^3)^{-1}$, being m_e^* the effective electron mass in the conduction zone. Then, we write the BE as

$$\frac{\partial n_k^e}{\partial t} = W_k^{(in)(\alpha)} (1 - n_k^e) - W_k^{(out)(\alpha)} n_k^e + G_{|\vec{k}|}^{PI} (1 - n_k^e) - W_k^{(exc)} n_k^e, \quad (1)$$

where $W_k^{(in)(\alpha)}$ is the electron inter- and intra-band scattering with other electrons and with phonons and $W_k^{(exc)}$ is the exciton formation [1]. Only the terms that are explicitly treated in this work although already included into the formalism described in [1, 2] will be described next.

3.1 Impact Ionization (II)

The impact ionization scattering rates (and the inverse process of Auger recombination) [3, 6, 8–10] are given by

$$W_k^{(in)(imp)} = \frac{2\pi}{\hbar} \sum_{\vec{k}', \vec{q}} |V^{(imp-in)}(q)|^2 (1 - n_{\vec{k}'} n_{\vec{k}-\vec{q}} n_{\vec{k}'+\vec{q}}) \times \delta(E_{\vec{k}} + E_{\vec{k}'} - E_{\vec{k}-\vec{q}} - E_{\vec{k}'+\vec{q}}), \quad (2)$$

$$W_k^{(out)(imp)} = \frac{2\pi}{\hbar} \sum_{\vec{k}', \vec{q}} |V^{(imp-out)}(q)|^2 n_{\vec{k}'} (1 - n_{\vec{k}-\vec{q}}) (1 - n_{\vec{k}'+\vec{q}}) \times \delta(E_{\vec{k}-\vec{q}} + E_{\vec{k}'+\vec{q}} - E_{\vec{k}} - E_{\vec{k}'}), \quad (3)$$

The static Thomas-Fermi screening effect is considered [11]

$$Q_s^2 = \frac{e^2}{\varepsilon_0 \varepsilon_r} \frac{m^*}{\pi^2 \hbar^2} (3\pi^2 n_{3D})^{1/3}, \quad (4)$$

where ε_r is the average dielectric constant of the material, and n_{3D} is the concentration of conduction electrons in the bulk material. The Coulomb scattering

potential is given by

$$V^{(imp-in)}(q) = \left(\frac{\pi\hbar}{\tilde{I}_0} \right)^{1/2} \left(\frac{qe^2}{\varepsilon_0\varepsilon_r(q^2 + Q_s^2)V} \right) \left(\frac{1}{m_{CB}^*} + \frac{1}{m_{VB}^*} \right)^{1/2}, \quad (5)$$

with effective ionization potential \tilde{I}_0 given in [5, 6].

3.2 Electron-Phonon Interaction

The electron scattering-in/scattering-out rates due to phonons, including phonon-assisted photon absorption are given by [2]:

$$\begin{aligned} W_k^{(in)(e-phn-pht)} &= \frac{2\pi}{\hbar} \sum_{\vec{q}, \lambda, M} |C_{\vec{q}\lambda}|^2 J_{|M|}^2 [\Gamma(q)] \\ &\times \left[n_{\vec{k}-\vec{q}} N_{\vec{q}\lambda}^{ph} \delta(E_{\vec{k}} - E_{\vec{k}-\vec{q}} - \hbar\omega_{\vec{q}\lambda} - M\hbar\Omega_L) \right. \\ &\left. + n_{\vec{k}+\vec{q}} (N_{\vec{q}\lambda}^{ph} + 1) \delta(E_{\vec{k}} - E_{\vec{k}+\vec{q}} + \hbar\omega_{\vec{q}\lambda} + M\hbar\Omega_L) \right], \quad (6) \end{aligned}$$

$$\begin{aligned} W_k^{(out)(e-phn-pht)} &= \frac{2\pi}{\hbar} \sum_{\vec{q}, \lambda, M} |C_{\vec{q}\lambda}|^2 J_{|M|}^2 [\Gamma(q)] \\ &\times \left[(1 - n_{\vec{k}+\vec{q}}) N_{\vec{q}\lambda}^{ph} \delta(E_{\vec{k}+\vec{q}} - E_{\vec{k}} - \hbar\omega_{\vec{q}\lambda} - M\hbar\Omega_L) \right. \\ &\left. + (1 - n_{\vec{k}-\vec{q}}) (N_{\vec{q}\lambda}^{ph} + 1) \delta(E_{\vec{k}-\vec{q}} - E_{\vec{k}} + \hbar\omega_{\vec{q}\lambda} + M\hbar\Omega_L) \right], \quad (7) \end{aligned}$$

where

$$\Gamma(q) = \frac{e |\vec{q} \cdot \vec{E}_L(t)|}{\sqrt{2} m^* \Omega_L^2}$$

and the contributions to the electron-phonon coupling constant come from optical phonons in the case of fused silica

$$|C_{qLO}|^2 = \left(\frac{\hbar\omega_{LO}}{2V} \right) \left(\frac{1}{\varepsilon_\infty} - \frac{1}{\varepsilon_0} \right) \frac{e^2}{\varepsilon_0 (q^2 + Q_s^2)},$$

where $\hbar\omega_{LO}$ is the optical phonon constant energy.

4 Lattice Temperature Evolution

Assuming, lattice quasi-equilibrium after every time step we can estimate the lattice temperature. The energy transferred to the lattice per unit time at each time step Δt results from the energy lost in the conduction band due to electron-phonon interaction:

$$\frac{\Delta E(t)}{\Delta t} = \int E dE \left[W_k^{(in)(e-phn-pht)} (1 - n_k^e) - W_k^{(out)(e-phn-pht)} n_k^e \right]. \quad (8)$$

Finally, ignoring space dependency the lattice temperature can be calculated [12] as follows

$$\rho C_p \frac{dT}{dt} = \frac{\Delta E(t)}{\Delta t} \quad (9)$$

ρ and C_p being the density and the heat capacity of the lattice, respectively.

5 Numerical Results for fs-Laser Irradiated Silica

We have applied the described formalism to fused silica. All parameters for the material used can be found in Ref. [4]. The detuning of the PI term from the bottom of the conduction band is calculated from Eq. (7) to be 500 meV with the magnitudes of the electron and hole effective masses chosen as half the free electron mass. The band gap energy is $E_G = 9$ eV and the optical phonon energy is $\hbar\omega = 153$ meV. The pulse temporal shape is taken to be a step function. The rest of the parameters are given in the captions of the figures. In the next examples, it is remarkable how obvious qualitative predictions can be accurately quantified with the BE model.

In Figure 1 is seen that the electron distribution curve peaks at 500 meV with PI included only, since this is the calculated detuning of the PI term from the bottom of the conduction band. In the other three curves (the included processes given in the caption) the initial peak diminishes and electron distribution is transferred to higher energy states, where peaks are observed at 2.5 eV, 5 eV, 7.5 eV *etc.* accompanied by small peaks as a result of the FCA process. It is also evident from the figure that the impact ionization leads to an appreciable increase of number of electrons at lower energies and the decrease of number of

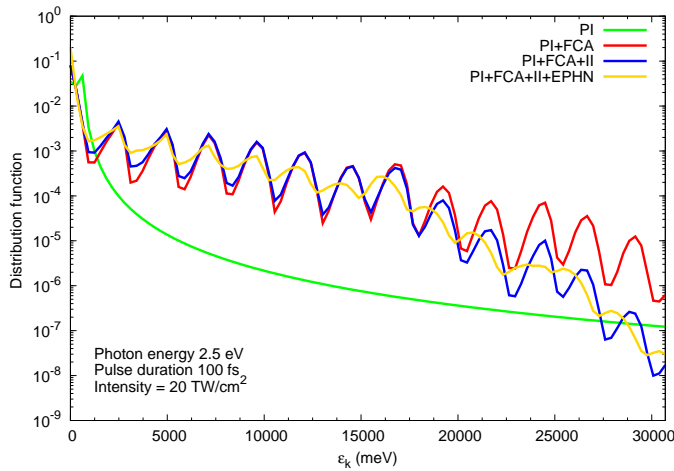


Figure 1. Electron energy distribution function as a function of electron energy for photon energy 2.5 eV.

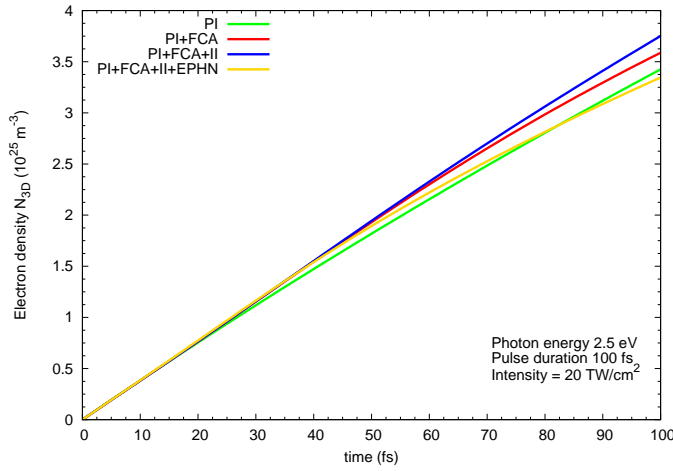


Figure 2. Electron density as a function of pulse duration for photon energy 2.5 eV.

electrons at higher energies. The effect of the electron-phonon (EP) scattering leads to decrease of the overall distribution function in comparison to its values when PI+FCA and PI+FCA+II processes are included since electrons tend to be scattered out of the high energy states that in turn weakens the effect of the other processes.

Figure 2 shows the evolution of electron density as a function of pulse duration for photon energy 2.5 eV when contributions from the processes of PI, FCA, II and EP are included. The density increase due to impact ionization as the pulse progresses is easily appreciated. Also the decrease of the electron density due to including EP interaction to the other processes is seen as a consequence of the predominant electron scattering out of higher energy states that decreases the effect of the impact ionization.

In Figure 3 the evolution of the average electron energy as a function of time is shown and it is clearly seen that the predominant electron scattering out of higher energy states due to EP process can be confirmed by comparing the curves where the processes of PI+FCA, PI+FCA+II and PI+FCA+II +EP are included. Also from comparing only the PI+FCA and PI+FCA+II curves we can conclude that for 2.5 eV laser pulse irradiation the effect of II is not that dramatic although significant.

Figure 4 illustrates the increase of lattice temperature due to the power transferred to the lattice due to electron-phonon scattering [Eq. (8)].

In Figure 5 the electron distribution function is depicted for photon energy of 5 eV and for the same processes included as in Figure 1. The curve representing the effect of PI peaks at a different energy due to the shift of detuning for higher photon energy and hence different number of photons involved in the photoionization. In the other three curves the initial peak diminishes and elec-

Simulation of Ultra-Intense Laser Irradiation Induced ...

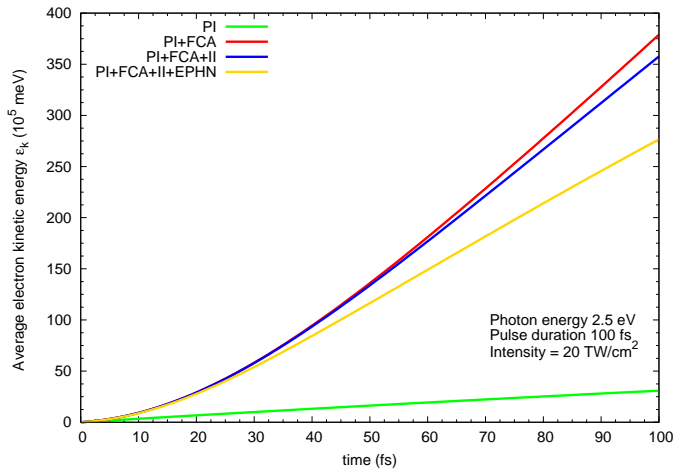


Figure 3. Electron average energy as a function of pulse duration for photon energy 2.5 eV.

tron distribution is transferred to higher energy states, where peaks are observed at 5 eV, 10 eV, 15 eV *etc.* as a result of the FCA process. It is also evident that the impact ionization leads to even more appreciable increase of number of electrons at lower energies and the decrease of number of electrons at higher energies in comparison with figure 1 while the electron-phonon (EP) interaction slightly lowers the magnitude of the distribution function uniformly in energy confirming that not so many electrons are scattered out of the higher energy states at 5 eV

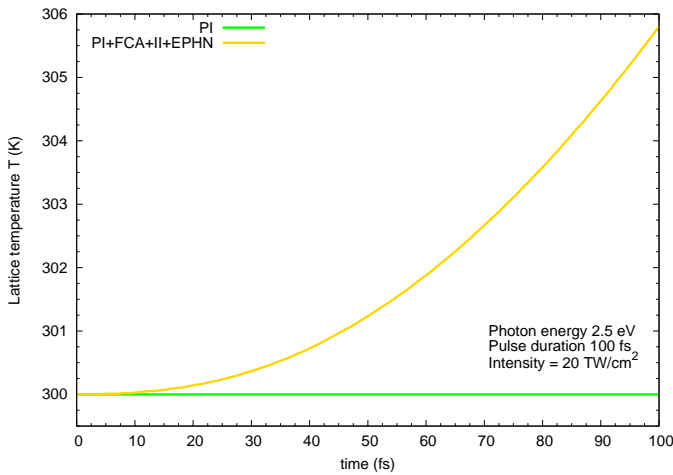


Figure 4. Lattice temperature as a function of pulse duration for photon energy 2.5 eV.

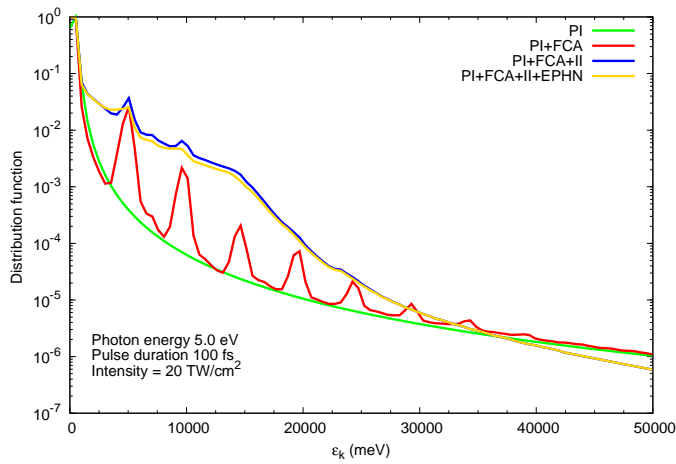


Figure 5. Electron energy distribution function as a function of electron energy for photon energy 5 eV.

photon energy and hence the effect of the impact ionization is almost unaltered by including the EP process.

Figure 6 shows the evolution of electron density as a function of pulse duration for photon energy 2.5 eV when contributions from the processes of PI, FCA, II and EP are included. The density increase due to impact ionization as the pulse progresses is very pronounced for this photon energy and the effect of electron-phonon interaction is also appreciable.

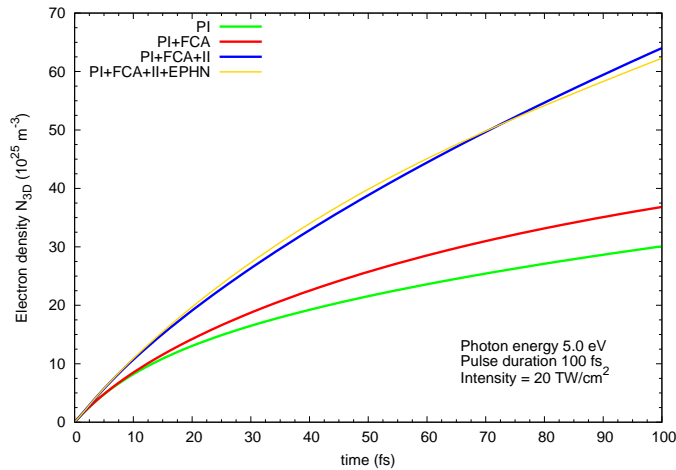


Figure 6. Electron density as a function of pulse duration for photon energy 5 eV.

Simulation of Ultra-Intense Laser Irradiation Induced ...

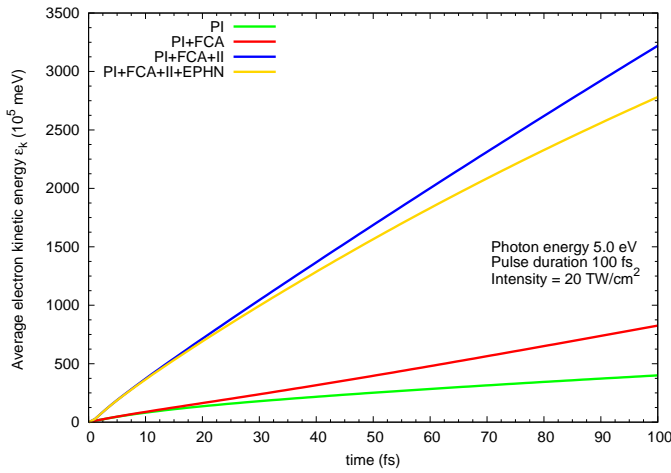


Figure 7. Electron average energy as a function of pulse duration for photon energy 5 eV.

In Figure 7 the evolution of the average electron energy as a function of time is shown and in this case the electron scattering out of higher energy states is not strong enhancing the effect of II. This can be confirmed by comparing the curves where the processes of PI+FCA+II and PI+FCA+II +EP are included. Also from comparing only the PI+FCA and PI+FCA+II curves we can conclude that for 5 eV laser pulse irradiation the effect of II is very significant.

Figure 8 illustrates the increase of lattice temperature due to electron-phonon coupling mechanism for the doubled photon energy. It is evident that the lattice

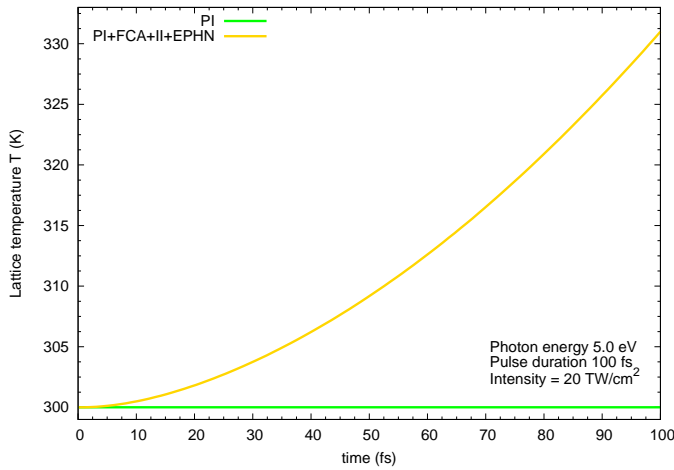


Figure 8. Lattice temperature as a function of pulse duration for photon energy 5 eV.

heating is much stronger in comparison to the case of the laser irradiation with 2.5 eV photon energy.

6 Conclusion

Ultra-short high laser intensity-induced electronic excitation in fused silica is modeled using a Boltzmann quantum kinetic formalism including photo-ionization, free carrier absorption of the electrons in the conduction band resulting in further absorption of laser energy and leading to impact ionization. Electron phonon scattering results in energy transfer to the lattice of the dielectric material. The transient conduction electron distribution function and integrated quantities such as electron density and the average electron energy during the irradiation are evaluated for two different photon energies (laser wavelengths) and for a 100 fs duration of the laser pulse. The heating of the lattice is also taken into account quantum mechanically based on the electron-phonon scattering rates. From the electron distribution function graphs we conclude that the high-energy electrons (the existence of a tail) resulting from the processes of PI and FCA are the determining factor underlying strong impact ionization effect. The laser radiation with higher photon energy leads to a stronger effect of the impact ionization because of the existence of higher energy electrons at the tail of the distribution and a lower rate of electron-phonon scattering out of these tail states in comparison to the case with twice as low photon energy. The graphs of the electron density and average electron energy evolution are another more quantitative argument confirming these conclusions. The effect of lattice heating due to electron-phonon scattering is stronger for 5 eV photon energy than for 2.5 eV photon energy of the laser irradiation. This is due to the enhancement of the microscopic processes taking place in the material for higher laser photon energy and the strong interplay between them.

Acknowledgements

The authors acknowledge funding by Spanish MINECO through the project MAT-2012-38541. T.A. acknowledges support from COST-STSM-MP-1208-04113-035409 and COST-STSM-MP-1208-120514-043832.

References

- [1] T. Apostolova, J.M. Perlado, A. Rivera, *Nucl. Instrum. Meth. B*, in print; ISSN: 0168-583X.
- [2] D. Huang, P.M. Alsing, T. Apostolova, D.A. Cardimona, *Phys. Rev. B* **71** (2005) 045204.
- [3] T. Apostolova, *Nucl. Instrum. Methods Phys. Res. Sect. Accel. Spectrometers Detect. Assoc. Equip.* **653** (2011) 72-75.
- [4] A. Kaiser, B. Rethfeld, M. Vicanek, G. Simon, *Phys. Rev. B* **61** (2000) 11437.
- [5] T.E. Itina, N. Shcheblanov, *Appl. Phys. Mater. Sci. Process.* **98** (2010) 769-775.

- [6] N. Shcheblanov, “Etude numérique des interaction d’un laser femtoseconde avec des cibles dielectriques: applications a la determination du seuil d’endommagement des composants optiques”, 2013.
- [7] T. Apostolova, D.H. Huang, P.M. Alsing, J. McIver, D.A. Cardimona, *Phys. Rev. B* **66** (2002) 075208.
- [8] W. Quade, E. Schll, F. Rossi, C. Jacoboni, *Phys. Rev. B* **50** (1994) 7398-7412.
- [9] J. Hader, J.V. Moloney, S.W. Koch, *IEEE J. Quantum Electron.* **41** (2005) 1217-1226.
- [10] J. Hader, J.V. Moloney, A. Thrnhardt, S.W. Koch, in: J. Piprek (Ed.), Nitride Semicond. Devices Princ. Simul., Wiley-VCH Verlag GmbH & Co. KGaA, (2007): pp. 145-167.
- [11] K. Sokolowski-Tinten, J. Bialkowski, A. Cavalleri, D. Von der Linde, A. Oparin, J. Meyer-ter-Vehn *et al.*, *Phys. Rev. Lett.* **81** (1998) 224-227.
- [12] C. Dufour, A. Audouard, F. Beuneu, J. Dural, J.P. Girard, A. Hairie, *et al.*, *J. Phys. Condens. Matter.* **5** (1993) 4573.